Supporting Information

Built-in electrical field enhanced ionic transport kinetics in T−Nb_2O_5@MoO_2 heterostructure

Huihuang Huang,[a] Guangyu Zhao,*[ab] Xin Sun,[a] Xianbo Yu,[a] Chao Liu,[a] Xiaojie Shen,[a] Ming Wang,[a] Pengbo Lyu*[c] and Naiqing Zhang*[ab]

[a] State Key Laboratory of Urban Water Resource and Environment, School of Chemistry and Chemical Engineering, Harbin Institute of Technology, Harbin 150001, China. E-mail: zhaogy810525@gmail.com; znqmww@163.com

[b] Academy of Fundamental and Interdisciplinary Sciences, Harbin Institute of Technology, Harbin 150001, China.

[c] Institut Charles Gerhardt Montpellier, UMR 5253, CNRS, Université de Montpellier, Montpellier, 34095, France. E-mail: pengbo.lyu@umontpellier.fr

Experimental section

All the chemical reagents were analytical grade and obtained commercially.

Synthesis of T−Nb_2O_5 nanorod array on niobium foil

Niobium foil was ultrasonically washed with acetone and water for several times and dried in vacuum oven. For synthesis of T−Nb_2O_5 nanorod array, 1.8 mmol of NH_4F was dissolved in 60 mL deionized water under stirring for several minutes, then the above solution and a piece of niobium foil (2 cm × 4 cm with a thickness of 200 μm, high temperature resistant polytetrafluoroethylene tape on one side) were transferred to 80 mL Teflon−lined autoclave. Afterwards, the autoclave was sealed and kept at 150 ℃ for 24 h. The obtained intermediate product was wash with water several times and dried at 60 ℃ in vacuum. Finally, the T−Nb_2O_5 nanorod array was obtained via heating treated at 750 ℃ for 2 h under Ar atmosphere. The resulted product is denoted as T−Nb_2O_5.

Synthesis of ammonium peroxo−polymolybdate aqueous solution

Typically, 3.0 g Mo powder was dissolved in 100 mL H_2O_2 at 60 ℃ via water bath. Until the powder was completely dissolved and cooled to room temperature, the excessive H_2O_2 was consumed by adding a Pt foil into solution. Finally, the solution was neutralized to pH = 7 with ammonia solution.

Synthesis of T−Nb_2O_5@MoO_2 nanorod array heterostructure on niobium foil

T−Nb_2O_5 nanorod array was dipped in ammonium peroxo−polymolybdate aqueous solution for 10 s, then the sample was dried at 60 ℃ in vacuum. Repeating the above process 5 times. Then the obtained sample was annealed at 550 ℃ for 2 h under Ar/H_2 atmosphere. The resulted product is denoted as T−Nb_2O_5@MoO_2.

Preparation of electrolytes

All the operation was executed in an argon−filled glove box (< 0.1 ppm of water and oxygen) at room temperature. The APC electrolyte for MRBs was prepared according to reported literature.[1] Firstly, 1.067 g aluminum chloride slowly dissolved in 12 mL THF under vigorous stirring and kept for 12 h. Subsequently, the transparent solution was added to 8 mL phenyl magnesium chloride (2 M in THF) dropwise under vigorous stirring and kept for another 12 h to obtain the 0.4 M APC electrolyte. Finally, 0.848 g anhydrous LiCl was dissolved in APC electrolyte to obtain 0.4 M APC–1.0 M LiCl electrolyte for MLIBs.

Material characterization

The morphology and microstructure of products were conducted by Field emission SEM (Hitachi, SU8010) with energy dispersive spectrometer (EDS) mapping and high resolution TEM (JEM–2100 with an accelerating voltage of 200 kV). The XRD patterns of products were characterized by PANalytical X'Pert PRO with Cu Kα radiation (λ=1.5418 Å). XPS was obtained by Thermo Fisher Scientific K−Alpha (Fisher Scientific Ltd, Nepean, ON).

Electrochemical characterization

The T−Nb_2O_5 and T−Nb_2O_5@MoO_2 were used as binder−free electrode directly.

Electrochemical performances of T−Nb_2O_5 and T−Nb_2O_5@MoO_2 were evaluated with 2025−type coin cell which were assembled in an argon−filled glove box, using Mg foil as the reference and counter electrodes. Microporous membrane (Celgard 2400) was employed as the separator. 0.4 M APC/THF and 0.4 M APC−1.0 M LiCl/THF were employed as the electrolyte of MRBs and MLIBs, respectively. Galvanostatic charge/discharge measurements were performed at ambient temperature by a battery test system (Shenzhen Neware Electronic Co., China) from 0.2−2.0 V vs Mg^{2+}/Mg. Cyclic voltammetry (CV) measurements were investigated by CHI 660D electrochemical workstation. Electrochemical impedance spectroscopy (EIS) measurements were conducted with Princeton Applied Research PARSTAT 2273 advanced electrochemical system with 5 mV amplitude, and the frequency range between 100 kHz and 0.1 Hz at open circuit potential. The mass loading of T−Nb_2O_5 and T−Nb_2O_5@MoO_2 heterostructure are about 1.20 and 1.29 mg cm^{-2}, respectively. Galvanostatic intermittent titration technique (GITT) was tested by a battery test system (Shenzhen Neware Electronic Co., China). GITT was conducted with a constant current pulse time of 20 min followed by a relaxation process of 60 min at a current density of 50 mA g^{-1}. The diffusion coefficient can be calculated by the following equation:[2]

$$D = \frac{4}{\pi\tau}\left(\frac{m_B V_M}{M_B S}\right)^2\left(\frac{\Delta E_s}{\Delta E_t}\right)^2 \#(1)$$

where τ represents the time of current pulse. m_B, V_M and M_B correspond to the mass, molar volume and molar mass of active materials, respectively. S is the contact area of electrode−electrolyte. ΔE_s and ΔE_t represent the potential change caused by the current pulse and potential change during the constant current charge/discharge.

Computational details

All calculations were carried out using the projector augmented wave (PAW)[3] formalism within the generalized gradient approximation (GGA) method with Perdew−Burke−Ernzerhof (PBE) exchange−correlation functional as implemented in Vienna Ab Initio Simulation Package (VASP).[4-6] The cutoff energy for the plane−wave basis set has been consistently set to 500 eV. The convergence criterion of 0.05 eV/Å and 10^{-4} eV were used for the forces and energy convergence in geometry

optimizations. The D3 correction[7] was employed to include the dispersion contribution for the adsorption. The transition states were localized using the climbing image nudged elastic band method (CI−NEB)[8] as implemented in the Transition State Tools for VASP (VTST) module. For the work function calculations, the vacuum was set to larger than 20 Å. Slab models have been used for T−Nb_2O_5 (1 0 0) and MoO_2 (−1 1 0) surface; the atoms of bottom three layers were fixed at the bulk values. The k−points were sampled with 2×2×1 Monkhorst−Pack grid for structure optimization and 6×6×1 for density of states (DOS).

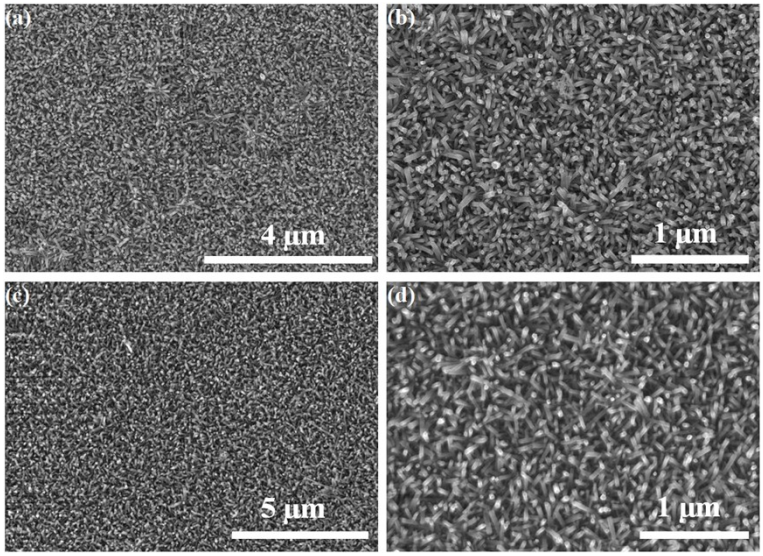

Figure. S1 SEM images of (a)(b) T−Nb_2O_5 precursor. (c)(d) T−Nb_2O_5.

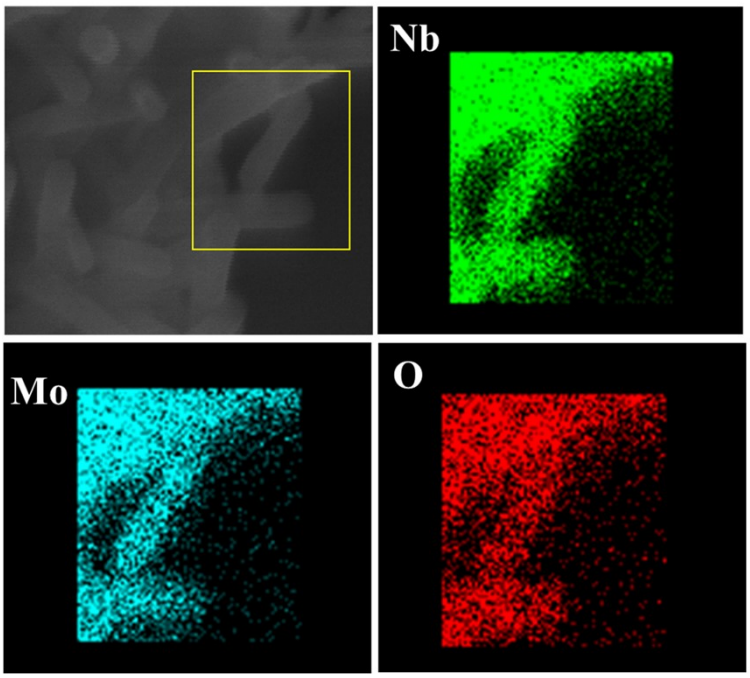

Figure. S2 EDS images of T−Nb_2O_5@MoO_2 heterostructure.

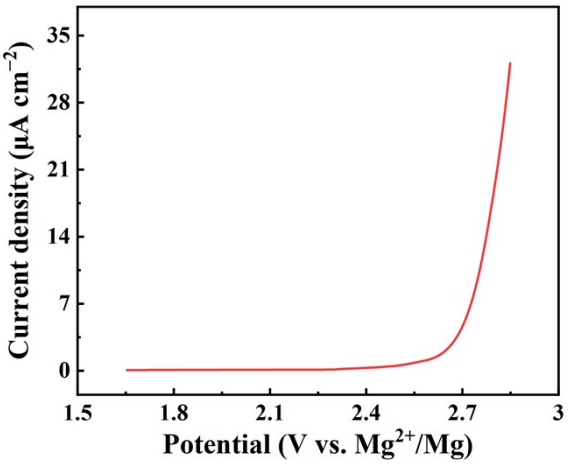

Figure. S3 Linear sweep voltammetry curve of niobium foil in APC-LiCl electrolyte at a scan rate of 1 mV s^{-1}.

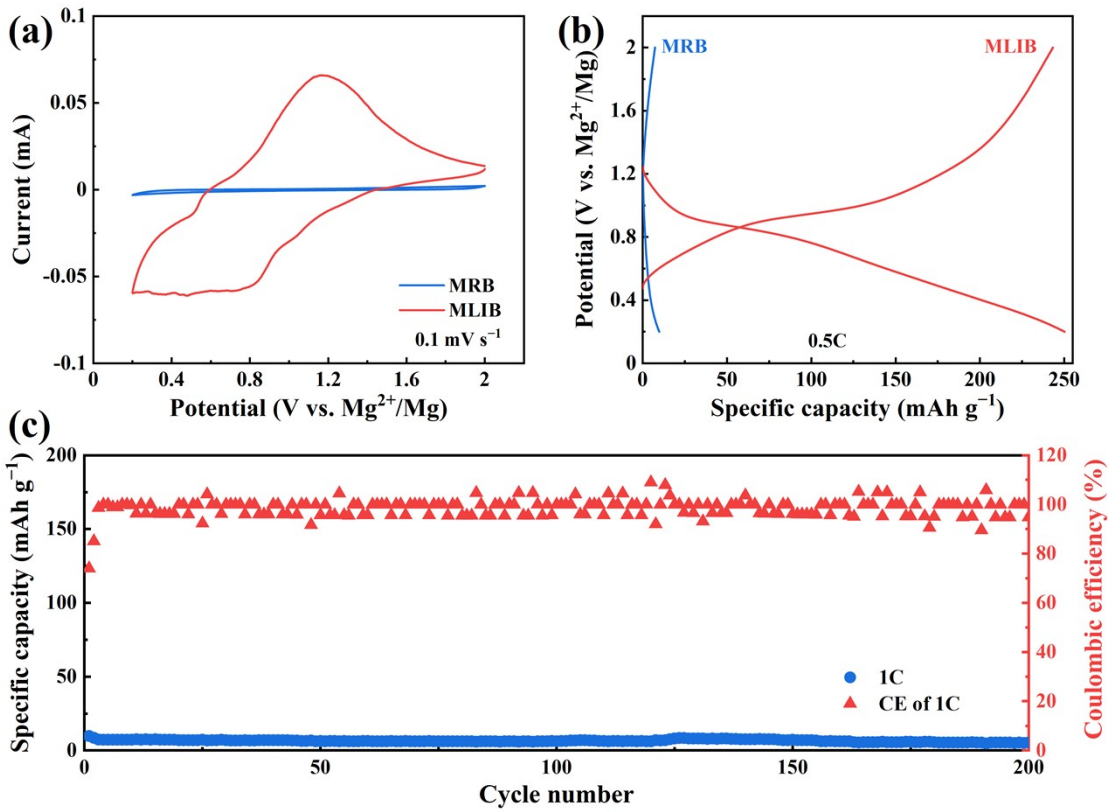

Figure. S4 The electrochemical measurement of T−Nb_2O_5@MoO_2 in MRB and MLIB: (a) CV curves, (b) galvanostatic charge/discharge curves, (c) the cycling performance at the current density of 1C in MRB.

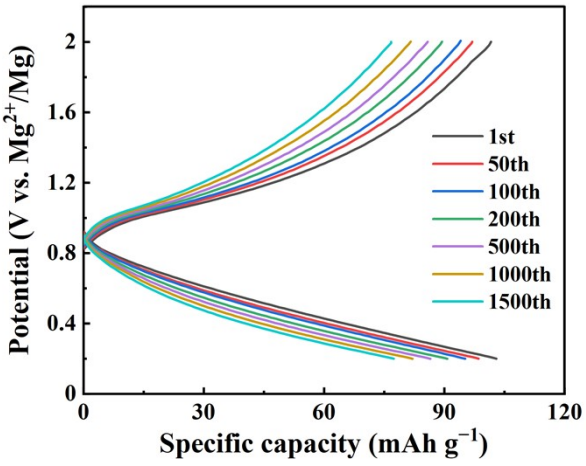

Figure. S5 The charge-discharge profiles of different cycles at a current density of 5C.

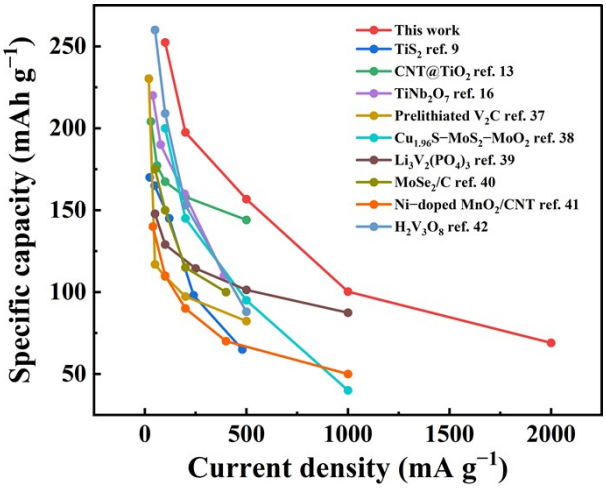

Figure. S6 The rate performance of T−Nb_2O_5@MoO_2 compares with other reported advanced electrode materials in MLIB.

Table. S1 Comparison of cycling stability of T−Nb_2O_5@MoO_2 with other reported advanced electrode materials for MLIB.

Materials	**Current Density (mA g^{-1})**	**Reversible Capacity (mA h g^{-1})**	**Cycle Number (n)**	**Retention**	**Reference**
T−Nb_2O_5@MoO_2 heterostructure	200	169.6	100	85.6%	This work
	1000	76.3	1500	75.9%	
V_2MoO_8	20	135.8	50	72.5%	*Nano Energy*, 2017, 34, 26[9]

$CNT@TiO_2$	30	161.9	100	69.3%	*J. Colloid Interface Sci.*, 2021, 581, 307[10]
$Cu_2S@C$	30	150.0	50	38.1%	*J. Power Sources*, 2020, 445, 227325[11]
VO_2	100	154.9	100	75.0%	*ACS Appl. Mater. Interfaces*, 2017, 9, 17060[12]
$H_2V_3O_8$	200	104.5	50	56.5%	*ACS Appl. Mater. Interfaces*, 2017, 9, 28667[13]
$MoSe_2/C$	200	89.0	100	57.4%	*Electrochem. Commun.*, 2018, 90, 16[14]
$Li_3V_2(PO_4)_3$	100	127.4	200	75.0%	*J. Mater. Chem. A*, 2019, 7, 9968[15]
$Cu_{1.96}S{-}MoS_2{-}MoO_2$	100	150.0	200	68.2%	*ACS Appl. Mater. Interfaces*, 2019, 11, 5966[16]
$MoS_2{-}CuS{-}EG$	50	172.4	200	47.4%	*Chem. Eng. J.*, 2021, 409, 128271[17]
T−Nb_2O_5 holey nanosheet	200	139.8	100	70.0%	*Nanoscale*, 2019, 11, 16222[18]
	1000	65.9	400	65.9%	

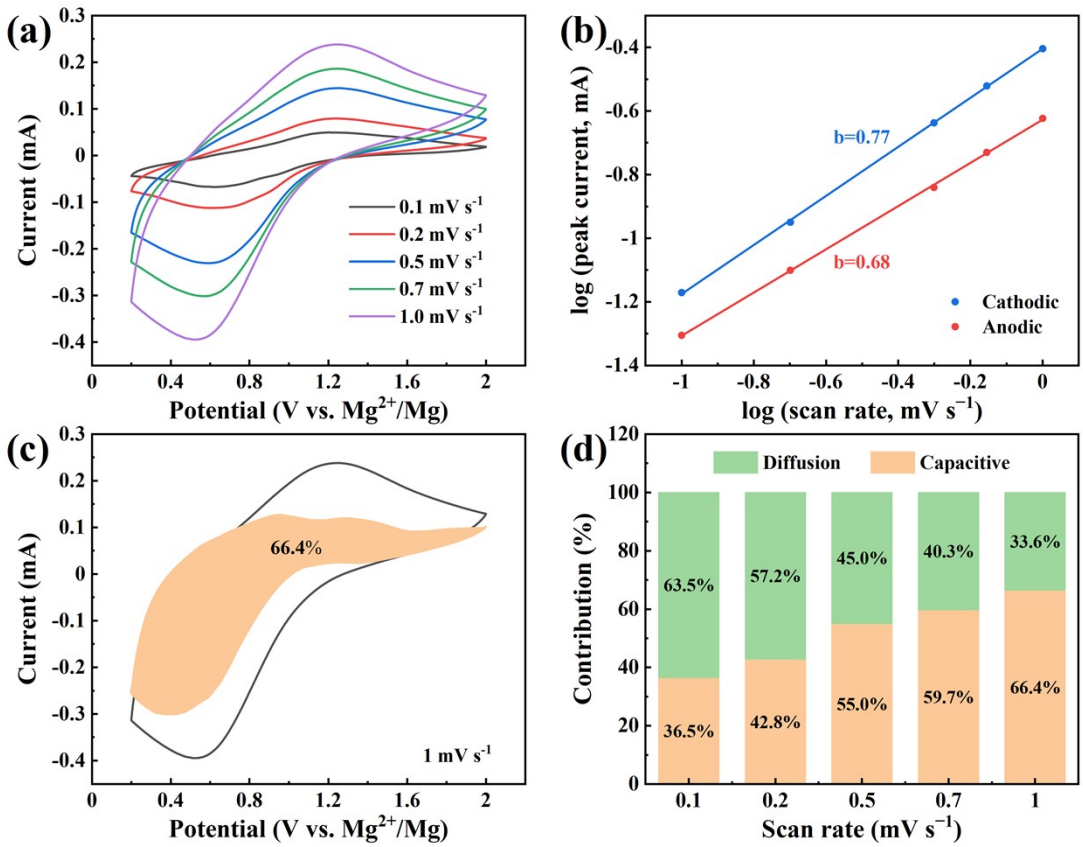

Figure. S7 The experimental analyses of electrochemical kinetics for T−Nb_2O_5 in MLIB: (a) CV curves at various scan rates, (b) the relationship between log (scan rate) and log (peak current) based on the CV curves at redox peaks, (c) the capacitive contribution at 1.0 mV s^{-1}, (d) corresponding capacitive and diffusion contributions at various scan rates.

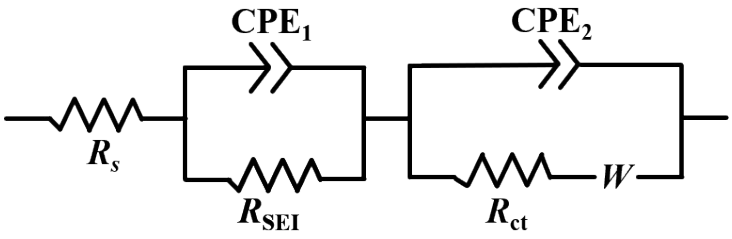

Figure. S8 The equivalent circuit model of Nyquist plots.

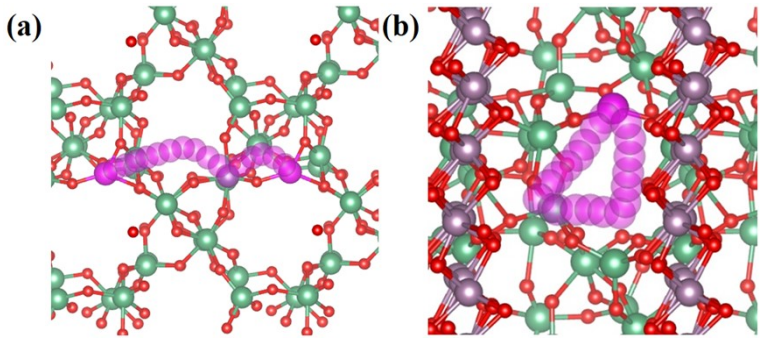

Figure. S9 The diffusion paths of Li^+ in (a) T−Nb_2O_5 surface and (b) T−Nb_2O_5@MoO_2 interface. The purple, red and green spheres stand for Mo, O and Nb atoms, respectively.

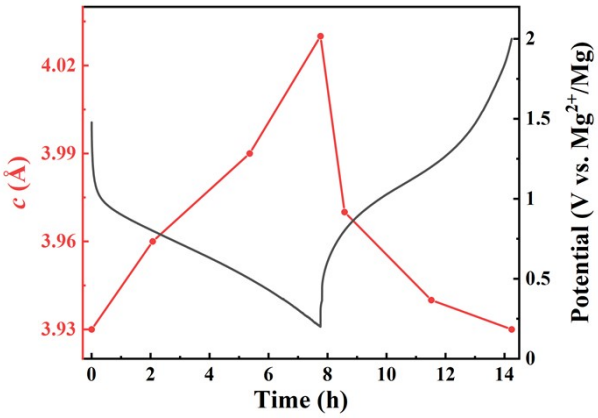

Figure. S10 The potential profile and the c-lattice parameter evolution process.

Reference

1. C. Liu, G. Zhao, L. Zhang, P. Lyu, X. Yu, H. Huang, G. Maurin, K. Sun and N. Zhang, *J. Mater. Chem. A*, 2020, **8**, 22712-22719.
2. P.-F. Wang, T. Jin, J. Zhang, Q.-C. Wang, X. Ji, C. Cui, N. Piao, S. Liu, J. Xu, X.-Q. Yang and C. Wang, *Nano Energy*, 2020, **77**, 105167.
3. J. P. Perdew, K. Burke and M. Ernzerhof, *Phys. Rev. Lett.*, 1996, **77**, 3865-3868.
4. P. E. Blöchl, *Phys. Rev. B*, 1994, **50**, 17953-17979.
5. G. Kresse and J. Furthmüller, *Comput. Mater. Sci*, 1996, **6**, 15-50.
6. G. Kresse and D. Joubert, *Phys. Rev. B*, 1999, **59**, 1758-1775.
7. S. Grimme, J. Antony, S. Ehrlich and H. Krieg, *J. Chem. Phys.*, 2010, **132**, 154104.
8. G. Henkelman, B. P. Uberuaga and H. Jónsson, *J. Chem. Phys.*, 2000, **113**, 9901-9904.
9. X. Miao, Z. Chen, N. Wang, Y. Nuli, J. Wang, J. Yang and S.-i. Hirano, *Nano Energy*, 2017, **34**, 26-35.
10. C. Zhu, Y. Tang, L. Liu, R. Sheng, X. Li, Y. Gao and Y. NuLi, *J. Colloid Interface Sci.*, 2021, **581**, 307-313.
11. W. Wang, Y. Yang, Y. NuLi, J. Zhou, J. Yang and J. Wang, *J. Power Sources*, 2020, **445**,

227325.
12. C. Pei, F. Xiong, J. Sheng, Y. Yin, S. Tan, D. Wang, C. Han, Q. An and L. Mai, *ACS Appl. Mater. Interfaces*, 2017, **9**, 17060-17066.
13. H. Tang, N. Xu, C. Pei, F. Xiong, S. Tan, W. Luo, Q. An and L. Mai, *ACS Appl. Mater. Interfaces*, 2017, **9**, 28667-28673.
14. J.-J. Fan, S.-Y. Shen, Y. Chen, L.-N. Wu, J. Peng, X.-X. Peng, C.-G. Shi, L. Huang, W.-F. Lin and S.-G. Sun, *Electrochem. Commun.*, 2018, **90**, 16-20.
15. M. Rashad, H. Zhang, X. Li and H. Zhang, *J. Mater. Chem. A*, 2019, **7**, 9968-9976.
16. C. Wu, J. Hu, J. Tian, F. Chu, Z. Yao, Y. Zheng, D. Yin and C. Li, *ACS Appl. Mater. Interfaces*, 2019, **11**, 5966-5977.
17. X. Hou, H. Shi, T. Chang, K. Hou, L. Feng, G. Suo, X. Ye, L. Zhang, Y. Yang and W. Wang, *Chem. Eng. J.*, 2021, **409**, 128271.
18. H. Huang, G. Zhao, N. Zhang and K. Sun, *Nanoscale*, 2019, **11**, 16222-16227.